Journal of Inflammation Research

Dovepress
Taylor & Francis Group

Open Access Full Text Article

ORIGINAL RESEARCH

Subchronic Chlorpyrifos Exposure Induces Thyroid Follicular Cell Pyroptosis to Exacerbate Thyroid Toxicity by Modulating Nrf2/Keap1/NF-κB Pathway in Male Mice

Bingyan Gu[1,*], Yuying Chen[1,*], Huifang Xu[2,*], Kunyu Zhan[3], Keying Zhu[3], Huan Luo[4], Yanqun Huang[5,*], Hanbing Zeng[3], Wenbiao Zheng[6], Kun Tian[7], Hongfeng Ruan[1]

[1]Institute of Orthopaedics and Traumatology, The First Affiliated Hospital of Zhejiang Chinese Medical University (Zhejiang Provincial Hospital of Chinese Medicine), Hangzhou, 310053, People's Republic of China; [2]Otolaryngology Department, The First Affiliated Hospital of Zhejiang Chinese Medical University (Zhejiang Provincial Hospital of Chinese Medicine), Hangzhou, 310053, People's Republic of China; [3]The Second Clinical Medical College, Zhejiang Chinese Medical University, Hangzhou, 310053, People's Republic of China; [4]Department of Pharmacy, The Second Affiliated Hospital, School of Medicine, Zhejiang University, Hangzhou, 310009, People's Republic of China; [5]The Affiliated Hangzhou Fuyang Hospital of TCM Orthopedics and Traumatology, Zhejiang Chinese Medical University, Hangzhou, 311400, People's Republic of China; [6]Department of Orthopedics, Taizhou Municipal Hospital, Taizhou, Taizhou, 318000, People's Republic of China; [7]Department of Orthopaedics, The Third Affiliated Hospital of Zhejiang Chinese Medical University, Hangzhou, 311400, People's Republic of China

*These authors contributed equally to this work

Correspondence: Huan Luo, Department of Pharmacy, The Second Affiliated Hospital, Zhejiang University School of Medicine, 88 Jiefang Road, Shangcheng District, Hangzhou, 310009, People's Republic of China, Email libra_rainbow@zju.edu.cn; Hongfeng Ruan, Institute of Orthopaedics and Traumatology, The First Affiliated Hospital of Zhejiang Chinese Medical University, 548 Binwen Road, Hangzhou, 310053, People's Republic of China, Email rhf@zcmu.edu.cn

Purpose: Chlorpyrifos (CPF), a widely used organophosphate pesticide in agriculture, particularly in China, has raised significant environmental and health concerns due to its persistence and bioaccumulation. While CPF-induced toxicity in multiple organ systems has been documented, its long-term impact on thyroid homeostasis and the underlying mechanisms remain poorly understood. This study aimed to investigate the subchronic effects of CPF on thyroid function and elucidate the underlying mechanisms of CPF-induced thyroid toxicity.

Methods: The study utilized 4-week-old male C57BL/6J mice as experimental subjects. These mice were exposed to CPF via intragastric gavage at doses of 3 or 6 mg/kg for a duration of 8 weeks. Throughout the study period, various parameters were assessed, including body weight, serum antioxidant capacity, thyroid endocrine function and structure, apoptosis markers, inflammatory cytokines, and relevant molecular pathways.

Results: The study revealed that CPF exposure resulted in significant systemic toxicity, manifested through reduced body weight and impaired serum antioxidant capacity. Examination of thyroid-specific effects showed disrupted thyroid endocrine function and structure, accompanied by increased apoptosis and elevated inflammatory cytokines. At the molecular level, CPF significantly stimulated thyroid follicle cell pyroptosis by upregulating the expression of Nlrp3, Caspase-1, and Gsdmd. Further mechanistic analysis demonstrated that CPF activated thyroid follicular cell pyroptosis by modulating the Nrf2/Keap1 antioxidative pathway and enhancing phosphorylation of p65 via NF-κB signaling.

Conclusion: This comprehensive investigation provides novel insights into the mechanisms of CPF-induced thyroid toxicity. The findings demonstrate that CPF exposure compromises thyroid homeostasis through the induction of follicular cell pyroptosis and modulation of the Nrf2/Keap1/NF-κB signaling axis, highlighting the potential health risks associated with CPF exposure and its impact on thyroid function.

Keywords: chlorpyrifos, thyroid toxicity, thyroid follicular cell, pyroptosis, Nrf2/Keap1/NF-κB pathway

Received: 20 February 2025
Accepted: 9 July 2025
Published: 15 July 2025

Graphical Abstract

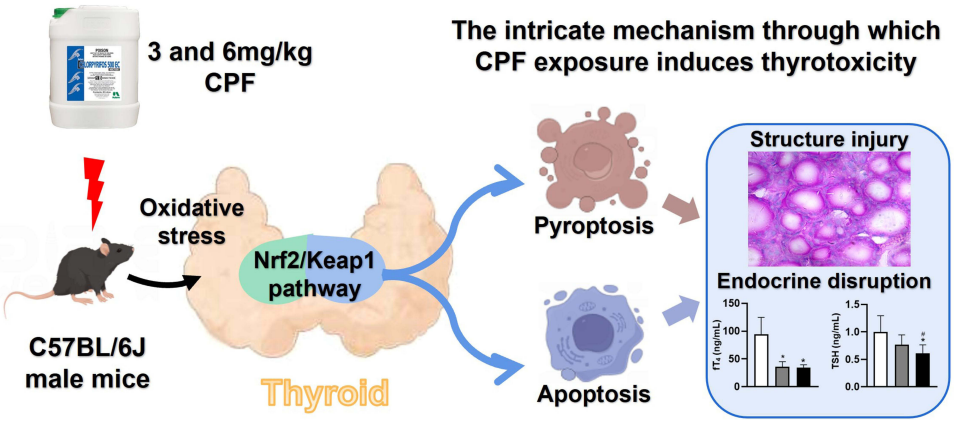

Introduction

Chlorpyrifos (CPF) is a broad-spectrum organophosphate pesticide widely used in agriculture and household pest control due to its high efficacy in eliminating various pests.[1] With global annual usage exceeding 200,000 tons in 2015 and continuing growth in demand,[2] its extensive application, particularly in rice, corn, wheat, and cotton cultivation, has led to widespread environmental contamination.[3] Given its stability in weakly acidic and neutral conditions and resistance to UV radiation, CPF residues have been extensively detected in multiple environmental matrices.[3] Decades of monitoring have revealed CPF contamination in seawater, rivers, groundwater, and even rainwater across different countries, with reported concentrations reaching 79.7 μg/L in surface water, frequently exceeding environmental allowable limits.[4] With a half-life ranging from 2.5 to 77 days,[5] CPF can persist in the environment and enter the human body through multiple exposure routes, including drinking water and food consumption,[6,7] raising serious concerns about its potential health impacts, as CPF toxicity has been associated with various chronic and acute diseases in humans and animals.

CPF is widely recognized for its toxic effects, which are primarily attributed to its inhibition of acetylcholinesterase (AChE), leading to acetylcholine accumulation and a spectrum of neurological symptoms, including pupil constriction, abdominal pain, bronchospasm, hypotension, bradycardia, salivation, tremors, seizures, and even coma.[8–10] It can also affect fetus, with a 65% frequency detection in human placentas, in North Patagonia.[11] In addition, CPF has been linked to endocrine disruption, affecting multiple organs, including the ovaries,[12] testes, pituitary tissues,[13] liver, and kidneys,[14] contributing to disorders in the thyroid,[15–18] sub-fertility/infertility,[19] breast cancer,[20] neurodevelopmental disorders,[21] and depression.[22] However, the long-term effects of CPF on thyroid structure and function and the underlying mechanisms remain inadequately characterized.

The thyroid gland is essential for metabolism and growth, primarily through secreting triiodothyronine (T_3) and thyroxine (T_4), with their free forms (fT_3 and fT_4) being the biologically active ones.[23] These hormones interact with thyroid-stimulating hormone (TSH) from the pituitary gland in a feedback loop: high fT_3 and fT_4 levels suppress TSH secretion, while low levels stimulate it, maintaining hormonal balance. The imbalance of trace elements such as environmental pollutants like cadmium (Cd) can lead to thyroid diseases, including Graves' disease, Hashimoto's thyroiditis, hypothyroidism, autoimmune thyroiditis, thyroid nodules, thyroid cancer and postpartum thyroiditis.[23] Structural alterations to thyroid follicles, such as changes in size, epithelial thickness, and colloid content, can disrupt hormone synthesis, leading to thyroid dysfunction or related disorders.[24,25] Numerous population-based studies have detected CPF derivatives in over 96% of urine samples tested, with higher levels in children, followed by adolescents, and lower levels in adults,[26,27] while acute CPF exposure among farmers has been associated with significant reductions in thyroid hormones, specifically fT_3 and total T_3, which correlate with elevated urinary CPF metabolites following pesticide spraying.[28] Moreover, increasing toxicological studies in rodents,[16,29–31] Xenopus laevis,[32] and Zebrafish[33]

further corroborate that both short- and long-term CPF exposure can disrupt thyroid function and structure, whereas the changes of thyroid hormones (T_3, T_4, and TSH) exposed to CPF are different or even contradictory, suggesting the need for deeper research into CPF's effects on thyroid homeostasis and the detailed molecular mechanism driving its toxicity.

Pyroptosis, a form of inflammatory cell death characterized by membrane pore formation and the release of pro-inflammatory cytokines, has emerged as a pivotal mechanism in toxicological responses.[34,35] This process is mainly driven by the Nod-like receptor protein 3 (Nlrp3) inflammasome, which activates Caspase-1, leading to the maturation of pro-IL-1β and pro-IL-18, as well as the cleavage of Gasdermin D (Gsdmd). The activated Gsdmd forms membrane pores, releasing intracellular contents and mature cytokines, IL-1β and IL-18, thereby amplifying inflammation.[36] Recent studies have linked NF-κB signaling-mediated thyroid follicular cell pyroptosis to the development of thyroiditis,[37] while environmental pesticide pollutants, including CPF, atrazine, and glyphosate, are found to stimulate Nlrp3-mediated pyroptosis in diverse cell types, such as epithelioma, keratinocyte HaCaT cells, cardiomyocytes, and renal tubular cells, contributing to tissue damage and toxicity in the skin, heart, and spleen.[35,38,39] Given these findings, it is plausible that CPF-induced thyroid toxicity may also involve thyroid follicular cell pyroptosis.

Oxidative stress is a major trigger for pyroptosis, with the nuclear factor E2-related factor 2 (Nrf2)/Kelch-like ECH-associated protein 1 (Keap1) pathway playing a central role in modulating oxidative stress responses and cellular homeostasis.[34,40] In response to oxidative stress, Nrf2 dissociates from Keap1 and translocates into the nucleus, where it activates genes containing antioxidant response elements in their promoters, such as heme oxygenase 1 (HO-1). Recent studies demonstrate that inhibition of Nrf2/Keap1 antioxidant pathway mediates cadmium-induced oxidative stress and thyroid follicular cell pyroptosis,[34] while enhancing Nrf2/Keap1 pathway activity mitigates pyroptosis in osteoblasts.[40] Moreover, CPF treatment has been shown to impair the Nrf2/Keap1 pathway, thereby inducing SH-SY5Y cell pyroptosis[41] and kidney injury.[42] However, it remains unclear whether CPF induces thyroid follicle cell pyroptosis via modulating the Nrf2/Keap1 antioxidant pathway.

Considering the environmental persistence of CPF, with residues widely detected in environmental samples and its potential health impacts, this study aimed to investigate the subchronic CPF exposure-induced thyrotoxicity at doses that did not cause acute death, which was adopted in previous studies[10,43,44] In this study, 4-week-old male C57BL/6J mice were divided into 3 groups and subjected to varying doses of CPF (0, 3, and 6 mg/kg, respectively) by gavage 5 times per week for 8 weeks. Body weight, serum antioxidant status, thyroid endocrine function and structure, and potential molecular alterations were evaluated. Our findings offer novel insights into CPF-induced thyrotoxicity, highlighting the potential role of follicular cell pyroptosis mediated by the Nrf2/Keap1/NF-κB signaling axis.

Materials and Methods

Chemicals and Reagents

Analytical grade CPF (CAS:2921–88-2, ≥ 99% purity) was obtained from Aladdin Bio-Chemical Technology Co., Ltd. (Shanghai, China). Assay kits for Malondialdehyde (MDA, A003–1–2), total antioxidant capacity (T-AOC, A015-1-2), glutathione peroxidase (GSH-Px, A005-1-2), Total superoxide dismutase (T-SOD, A001-3), fT_3 (H222), fT_4 (H223), TSH (H087–1–2) were provided by Nanjing Jiancheng Bioengineering Institute (China). PAS staining kit (GLYCOPRO-1KT) was supplied by Solarbio (Beijing, China). The antibodies used in this study are listed in Table 1. Vector TrueVIEW Autofluorescence Quenching Kit (SP-8500-15) was from Vector Laboratories Inc (Newark, USA). The TUNEL BrightGreen Apoptosis Detection Kit was purchased from Vazyme Biotech (Nanjing, China). Unless otherwise indicated, all other reagents were supplied by Sigma-Aldrich (St. Louis, MO).

Animals and Treatments

A total of 18 male C57BL/6J mice (4-week-old, weighing 10–16 g) were obtained from the Animal Experiments Center of Zhejiang Chinese Medical University (Grade SPF, SCXK (Shanghai)). All mice were housed in a specific pathogen-free condition at 23 ± 2 °C with a 12-hour light/dark cycle and provided with free access to water and standard lab chow. The standard experimental diet comprised moisture ≤ 10%, crude protein ≥ 18%, crude fat ≥ 4%, crude fiber ≤ 5%, and crude ash ≤ 8% (Shenyang Maohua Biotechnology Co., Ltd., Shenyang Province, China). No CPF exposure occurred in the environment or

Table 1 Detailed Information of Antibodies Used in This Study

Antibody	Host Species	Dilution	Catalog #	Company
Caspase-3	Rabbit	1:400	RLM3431	Ruiying biological
IL-1β	Rabbit	1:300	RLT4001	Ruiying biological
IL-18	Rabbit	1:400	RLN1926	Ruiying biological
Tnf-α	Rabbit	1:400	RLT4689	Ruiying biological
Nlrp3	Rabbit	1:400	19771-1-AP	Proteintech
Caspase-1	Rabbit	1:300	22915-1-AP	Proteintech
Gsdmd	Rabbit	1:400	ab219800	Abcam
Nrf2	Rabbit	1:400	YT3189	Immunoway
Keap1	Rabbit	1:300	YT5218	Immunoway
HO-1	Rabbit	1:400	10701-1-AP	Proteintech
p-p65	Rabbit	1:300	RLP0191	Ruiying biological

diet. All experimental protocols for mouse procedures were approved by The Committee on The Ethics of Animal Experiments of Zhejiang Chinese Medical University (Approval No. 20211227–03) and were conducted in accordance with the ARRIVE Guidelines and the 3Rs principles (Replacement, Reduction, and Refinement) for animal welfare.

Given the potential CPF-induced thyrotoxicity and acute oral LD_{50} of CPF (60 mg/kg) in mice in previous studies,[16,30,45,46] experimental doses of 3 and 6 mg/kg (1/20 and 1/10 of the LD_{50}) were selected for the present study, which aligns with reported exposure levels in occupational settings involving organophosphate pesticides.[47–50] All mice were randomly divided into 3 groups (n = 6 in each group): Vehicle group, Low-dose CPF exposure group, and High-dose CPF exposure group. CPF was administered via intragastric gavage at 3 or 6 mg/kg CPF, 5 times per week, while the Vehicle group received an equal volume of corn oil. After 8 weeks of treatment, all mice were anesthetized with 2% sodium pentobarbital (40 mg/kg), and blood was first collected via abdominal aortic function, then centrifuged at 3000 rpm for 10 minutes at 4°C to separate serum from cellular components. The resulting serum was immediately processed for analysis or stored at −80°C until use.

The thyroid isolation procedure began with a midline cervical incision to expose the submandibular gland, which was carefully reflected upward to reveal the underlying thyroid cartilage and trachea. Using microdissection techniques with ophthalmic scissors, we meticulously removed the overlying ventral musculature and fascial layers to fully expose the thyroid cartilage. With the anatomical structures clearly visualized, curved ophthalmic forceps were inserted beneath the thyroid cartilage to gently elevate the cartilage-tracheal complex.[34]

Serum Indicator Analysis

Serum levels of thyroid hormones (fT_3, fT_4, and TSH) were measured using corresponding ELISA kits, according to the manufacturer's instructions. The serum capacities of MDA, SOD, T-AOC, and GSH-Px were assessed using respective commercial assay kits.

Histological, Immunofluorescence (IF) and Immunohistochemistry (IHC) Analyses

After fixation in 4% formaldehyde, thyroid was dehydrated in 30% sucrose solution, embedded in OCT (Sakura Finetek, Japan), and sectioned at 8 μm thickness. HE staining and PAS staining were performed to analyze tissue morphology, and images were captured using a Carl Zeiss light microscopy (Göttingen, Germany) at 20× magnification. The diameter of the follicles (DF) was calculated by averaging the length of the lines through the follicle center in four directions (0°, 45°, 90°, 135°), denoted as a1 to a4, using the formula:

$$DF = (a1 + a2 + a3 + a4)/4$$

Follicle diameter was calculated by selecting 6 follicles per section across 4 random visual fields. The number of follicles was counted within a defined area (for follicles crossing the margin, only those with more than half of their area

were counted). The average height of thyroid follicular epithelial cells was measured in 6 randomly selected follicles, with results expressed in micrometers.

For IF analysis, sections were blocked with 5% normal goat serum for 1 hour at room temperature, followed by incubation with primary antibodies targeting Caspase-3, IL-1β, Nlrp3, Caspase-1, Gsdmd, Nrf2, Keap1, HO-1, and p-p65 at 4°C overnight. Subsequently, sections were incubated with a Dylight 488-conjugated secondary antibody (1:400, ImmunoWay, RS23220) for 1 hour at 37°C in the dark, and nonspecific fluorescence was quenched using the Vector TrueVIEW Autofluorescence Quenching Kit. IF images were captured with a Carl Zeiss fluorescence microscope (Göttingen, Germany). For IHC analysis, sections were blocked with PBS containing 5% normal goat serum for 30 minutes and incubated with the corresponding primary antibody (IL-18 and Tnf-α) at 4°C overnight. The following day, sections were treated with a rabbit-enhanced polymer detection system (PV9001, Zhongshan Golden Bridge Biotechnology, China) for 30 minutes, followed by visualization with 0.05% diaminobenzidine (DAB). Images were captured with a Carl Zeiss microscope. Each experiment was performed in triplicate, and quantitative histomorphometric analyses were conducted in a blinded manner using Image-Pro Plus Software version 6.0 (Media Cybernetics Inc, Rockville, Maryland, USA).

Quantitative histomorphometric analysis was performed using Image-Pro Plus Software version 6.0 (Media Cybernetics Inc., Rockville, MD, USA) in a blinded manner, following the previously outlined methodology.

Tunel Assay

Apoptotic cells in situ were identified using the TUNEL Bright Green Apoptosis Detection Kit according to the manufacturer's instructions. Negative controls were prepared by substituting the TdT enzyme solution with PBS. Positive cells were quantified in 6 randomly selected samples from each group. Nuclei were counterstained with DAPI, and the total number of cells was recorded.

Statistical Analysis

All numerical data are presented as mean ± SEM. Statistical analyses were performed using GraphPad Prism 8 software (GraphPad Software Inc., La Jolla, CA). The differences between multiple groups were analyzed using One-way analysis of variance (ANOVA) followed by Tukey's post-hoc test. $P < 0.05$ was considered statistically significant.

Results

CPF Exposure Induces Systemic Toxicity in Mice

To better understand the chronic systemic toxicity induced by CPF, we first assessed the final body weight in mice after 8 weeks of treatment. Administration of CPF led to a reduction in body weight in both the 3 mg/kg and 6 mg/kg CPF groups (Figure 1A). The systemic toxicity of CPF was further evaluated by measuring key serum antioxidant markers, including GSH-Px, T-AOC, SOD, and MDA. The results showed that CPF treatment significantly decreased serum GSH-Px activity, with the 6 mg/kg group showing a more pronounced reduction compared to controls (Figure 1B). T-AOC levels were significantly reduced in the high-dose CPF group (6 mg/kg) compared to the vehicle control (Figure 1C). In contrast, while SOD levels showed a trend toward reduction, and MDA levels tended to increase, neither change reached statistical significance (Figure 1D–E), suggesting that while oxidative stress is apparent, certain oxidative markers like SOD and MDA may be less sensitive to CPF's effects or may require longer exposure for significant alterations to manifest. Collectively, these findings highlight CPF's role in inducing systemic toxicity and disrupting oxidative balance in a dose-dependent manner.

CPF Exposure Disrupts Thyroid Endocrine Function and Damages Morphological Structure

To evaluate the toxic effect of CPF on thyroid endocrine function, we quantified serum levels of thyroid hormones. CPF treatment led to significant reductions in both fT_4 and TSH levels (Figure 2A). Specifically, CPF at 3 and 6 mg/kg resulted in a 62.3% and 19.4% decrease in fT_4, and a 13.5% and 51.9% reduction in TSH levels, respectively, suggesting that subchronic CPF exposure disrupts thyroid function.

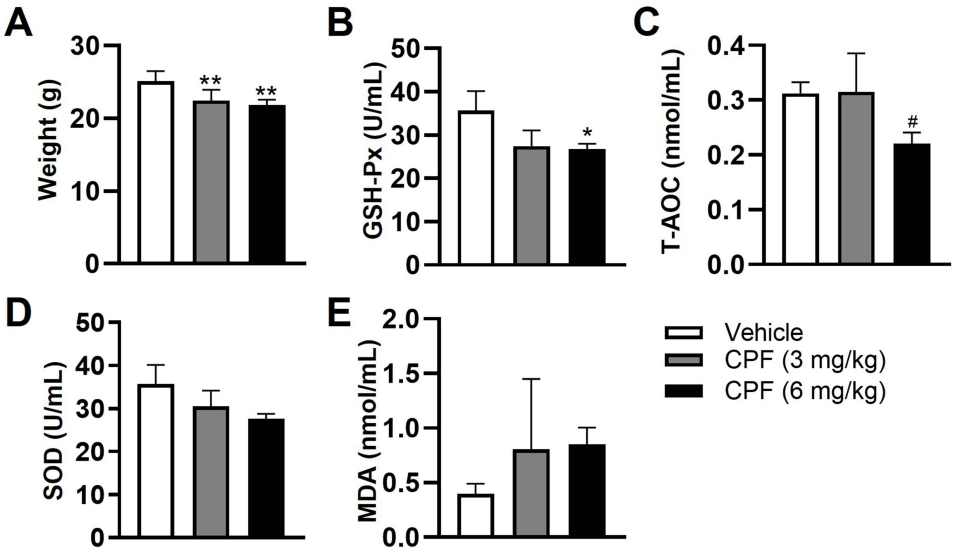

Figure 1 Effects of CPF exposure on body weight and serum antioxidant capacity in mice. (**A**) Effects of CPF exposure on body weight after 8 weeks of CPF treatment. (**B**–**E**) The amount of GSH-Px activity (**B**), T-AOC (**C**), SOD (**D**), and MDA (**E**) in the serum of mice after 8 weeks of CPF exposure. Data are presented as mean ± SEM. Each experiment was performed in triplicate. Statistical analysis was performed using one-way ANOVA followed by Tukey's post-hoc test. $^{*}P < 0.05$, $^{**}P < 0.01$ (vs vehicle group), $^{\#}P < 0.05$ (vs 3 mg/kg CPF group), n = 6 per group.

Abbreviations: CPF, Chlorpyrifos; GSH-Px, Glutathione peroxidase; T-AOC, Total antioxidant capacity; SOD, Superoxide dismutase; MDA, Malondialdehyde; SEM, Standard error of mean; ANOVA, Analysis of variance.

Histological examination using HE staining and PAS staining revealed that CPF-treated groups exhibited a gradual reduction in follicle volume, with varying degrees of shape irregularities, increased follicular epithelial thickness, and inflammatory cell infiltration (Figure 2B–D). Additionally, the colloid within thyroid follicles was markedly reduced (Figure 2C). These observations suggest that CPF exposure induces structural damage to the thyroid gland.

CPF Exposure Promotes Thyroid Follicular Cell Apoptosis in Mice

To evaluate the effects of CPF exposure on thyroid follicle cell apoptosis, IF analysis of Caspase-3, a specific apoptosis marker, and Tunel staining analysis were conducted. The results indicated a dose-dependent increase in Caspase-3 expression under CPF exposure. Specifically, the 3 mg/kg group exhibited higher Caspase-3 expression than the 6 mg/kg group (Figure 3A and B). In parallel, Tunel staining revealed a substantial increase in the number of Tunel-positive cells in CPF-treated mice compared to the vehicle mice (Figure 3C and D).

CPF Exposure Enhances Inflammatory Response in Thyroid Tissue

To assess whether CPF administration affects inflammatory response in the thyroid, we determined the expression of inflammatory factors, including IL-1β, IL-18, and Tnf-α, using IF or IHC assay. The expression of those factors was significantly enhanced in CPF-treated mice in a dose-dependent manner (Figure 4A–F). Notably, 6 mg/kg CPF exposure led to an 82.4-fold increase in IL-1β, surpassing the increases seen in other inflammatory cytokines (Figure 4A–F), indicating a potentially critical role of IL-1β in the CPF-induced thyrotoxicity.

CPF Exposure Activates Thyroid Follicular Cell Pyroptosis in Thyroid Tissue

Given the well-established role of IL-1β in thyroid toxicity and its maturation via inflammasomes, the molecular mechanism of Nlrp3 inflammasome-mediated thyroid follicle cell pyroptosis has garnered considerable attention in the context of thyroid disorders.[34,51] To determine whether the thyroid follicle cell pyroptosis participates in CPF-induced thyroid toxicity, the expression of pyroptosis-related proteins, including Nlrp3, Caspase-1, and Gsdmd, was examined using IF assay. Consistent with our previous findings,[34,35] the expression levels of Nlrp3, Caspase-1, and Gsdmd, were elevated by 11.7- and 33.4-fold, 15.9- and 31-fold, and 16.9- and 39.5-fold, respectively (Figure 5A–F). These results

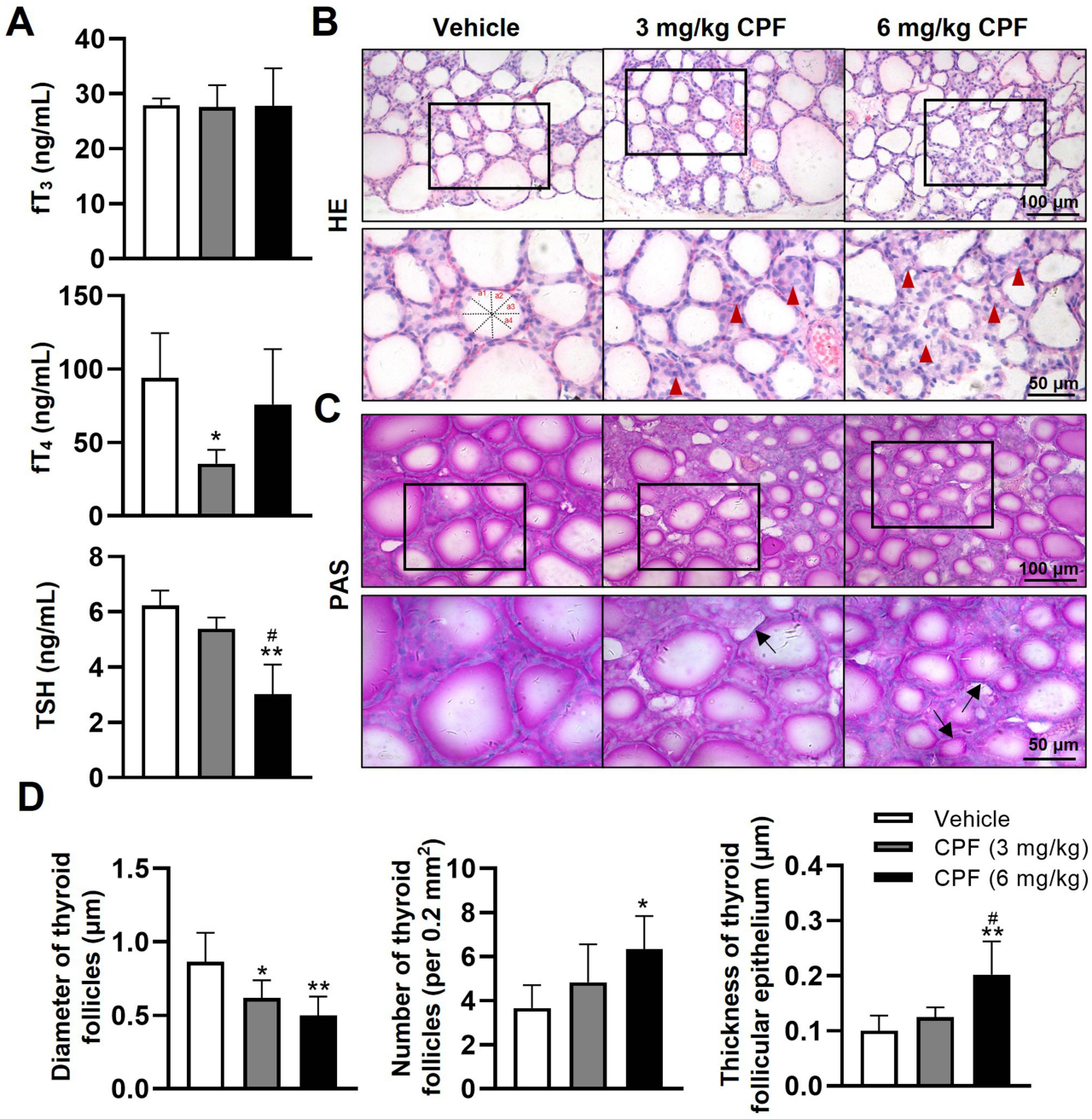

Figure 2 Effects of CPF exposure on thyroid hormone levels and histological structure. (**A**) Serum levels of thyroid hormones, including fT_3, fT_4, and TSH, were measured after 8 weeks of CPF exposure. (**B** and **C**) Representative histological images of thyroid tissues stained with HE (**B**) and PAS (**C**). Red arrows in (**B**) indicate typical inflammatory infiltration in thyroid. Black arrows in (**C**) indicate structural changes such as follicular cells and reduced colloid content. (**D**) Quantitative analysis of thyroid follicular characteristics, including follicle diameter, follicle number (per 0.2 mm^2), and epithelial thickness. The diameter of the follicle was calculated by averaging the length of the line through the center of the follicle in four directions (0°, 45°, 90°, 135°). *DF* = (a1+a2+a3+a4)/4. Data are shown as mean ± SEM. All experiments were performed in triplicate. Statistical analysis was performed using one-way ANOVA followed by Tukey's post-hoc test. $^{*}P < 0.05$, $^{**}P < 0.01$ (vs vehicle group), $^{\#}P < 0.05$ (vs 3 mg/kg CPF group), n = 6 per group.

Abbreviations: CPF, Chlorpyrifos; fT3, Free triiodothyronine; fT4, Free thyroxine; TSH, Thyroid-stimulating hormone; HE, Hematoxylin and eosin; PAS, Periodic Acid-Schiff; SEM, Standard error of mean; ANOVA, Analysis of variance.

demonstrate that CPF may enhance excessive production of inflammatory cytokines, primarily through the activation of Nlrp3-mediated pyroptosis in thyroid follicular cells.

CPF Exposure Modulates the Nrf2/Keap1/NF-κB Pathway

To elucidate the molecular mechanisms underlying CPF-induced pyroptosis in thyroid follicular cells, we investigated the activity of the Nrf2/Keap1 antioxidant pathway and downstream NF-κB pathway by determining the expression of Nrf2,

https://doi.org/10.2147/JIR.S523861

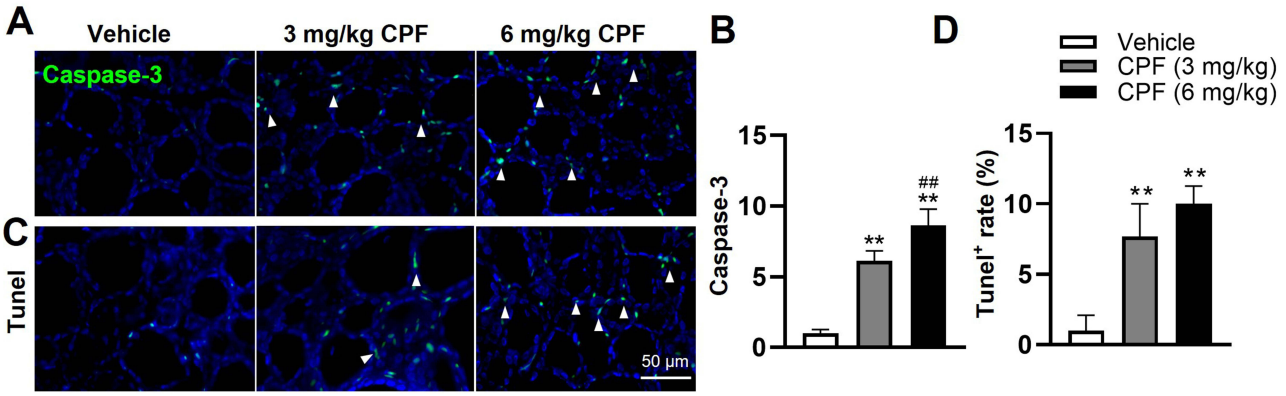

Figure 3 CPF exposure induces apoptosis in thyroid follicular cells. (**A**) Representative IF images showing Caspase-3 (green) expression in thyroid tissues after 8 weeks of CPF exposure. DAPI (blue) was used to counterstain nuclei. White arrowheads indicate Caspase-3-positive cells. (**B**) Quantitative analysis of Caspase-3-positive cells in thyroid tissues. (**C**) Representative TUNEL staining images of thyroid tissues. TUNEL-positive cells are indicated by white arrowheads. (**D**) Quantification of TUNEL-positive cells in thyroid tissues, expressed as the percentage of total cells. Data are presented as mean ± SEM. All experiments were performed in triplicate. Statistical analysis was performed using one-way ANOVA followed by Tukey's post-hoc test. $^{**}P < 0.01$ (vs vehicle group), $^{\#\#}P < 0.01$ (vs 3 mg/kg CPF group), n = 6 per group.
Abbreviations: CPF, Chlorpyrifos; IF, Immunofluorescence; DAPI, 4′,6-diamidino-2-phenylindole; TUNEL, Terminal deoxynucleotidyl transferase dUTP nick end labeling; SEM, Standard error of mean; ANOVA, Analysis of variance.

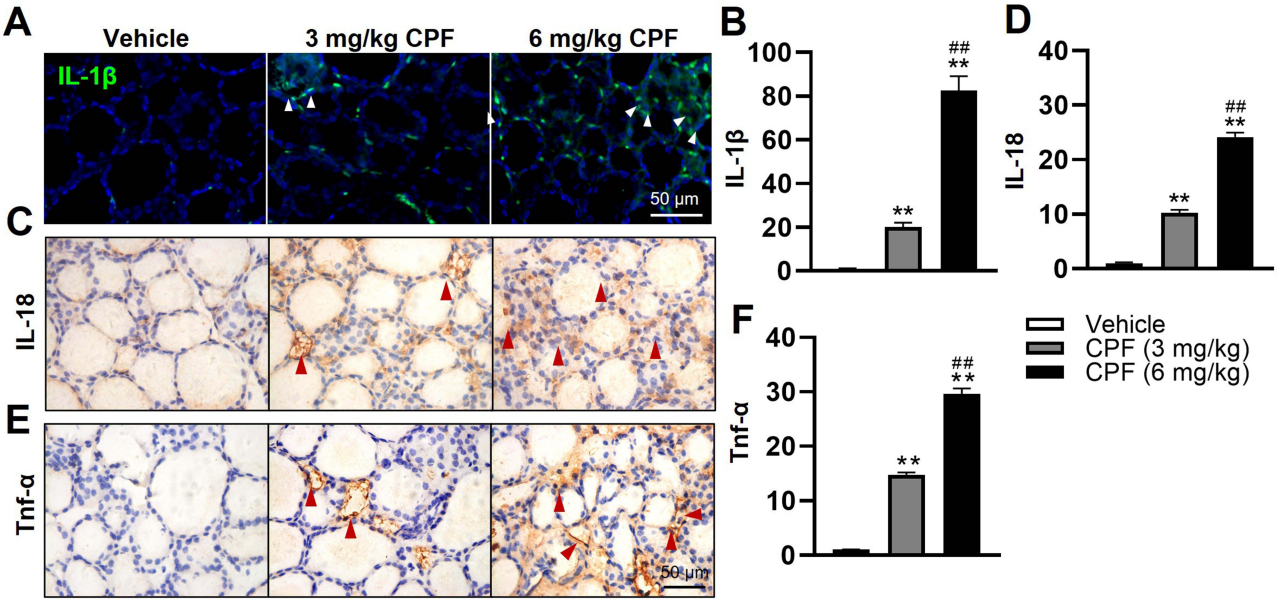

Figure 4 CPF exposure promotes inflammatory cytokine production in thyroid tissues. (**A**) Representative IF images showing IL-1β (green) expression in thyroid tissues. DAPI (blue) was used to counterstain nuclei. White arrowheads indicate IL-1β-positive cells. (**B**) Quantitative analysis of IL-1β expression in thyroid tissues. (**C**) Representative IHC images of IL-18 expression (brown) in thyroid tissues. Red arrowheads indicate IL-18-positive cells. (**D**) Quantitative analysis of IL-18 expression in thyroid tissues. (**E**) Representative IHC images of TNF-α expression (brown) in thyroid tissues. Red arrowheads indicate TNF-α-positive cells. (**F**) Quantitative analysis of TNF-α expression in thyroid tissues. Data are presented as mean ± SEM. All experiments were performed in triplicate. Statistical analysis was performed using one-way ANOVA followed by Tukey's post-hoc test. $^{**}P < 0.01$ (vs vehicle group), $^{\#\#}P < 0.01$ (vs 3 mg/kg CPF group), n = 6 per group.
Abbreviations: CPF, Chlorpyrifos; IF, Immunofluorescence; DAPI, 4′,6-diamidino-2-phenylindole; IL-1β, Interleukin-1 beta; IL-18, Interleukin-18; IHC, Immunohistochemistry; TNF-α, Tumor necrosis factor alpha; SEM, Standard error of mean; ANOVA, Analysis of variance.

Keap1, and HO-1, as well as the phosphorylated status of p65 (p-p65, indicator of NF-κB pathway activity) using IF analysis. As depicted in Figure 6A–D, we found that CPF significantly increased the expression of Keap1 and p-p65 while decreasing the expression of Nrf2 and HO-1 in a dose-dependent manner. Taken together, these results suggest that CPF might augment thyroid follicular cell pyroptosis by modulating Nrf2/Keap1/NF-κB pathway, thereby exacerbating thyroid toxicity.

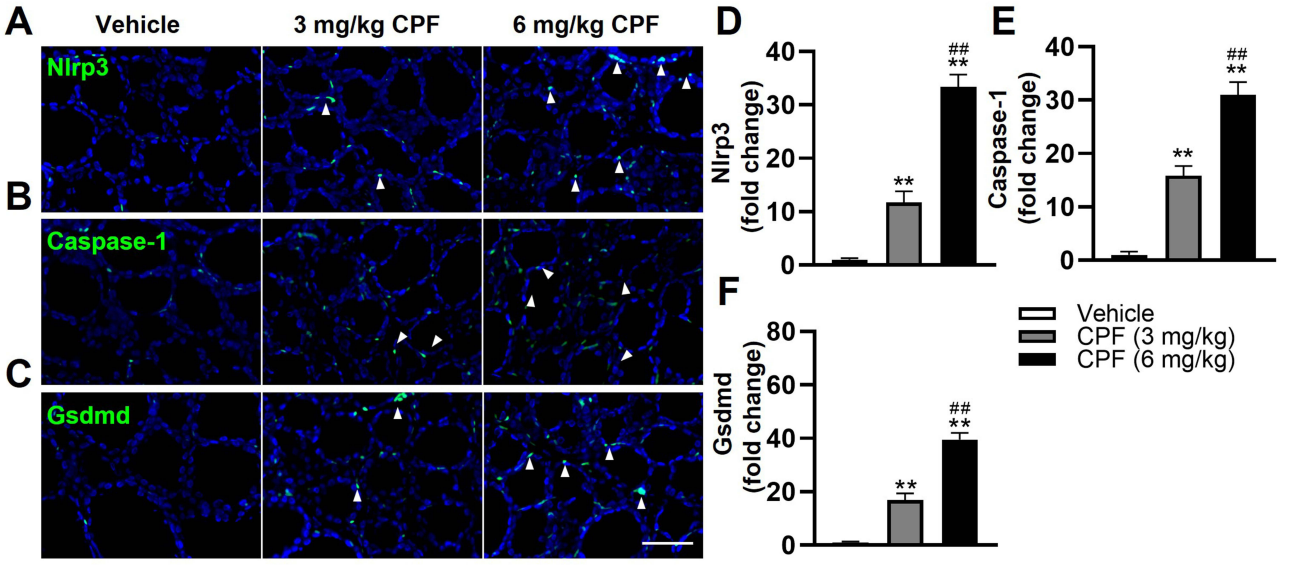

Figure 5 CPF exposure activates thyroid follicular cell pyroptosis in mice. (**A**–**C**) Representative IF images showing the expression of pyroptosis-related proteins (Green), including Nlrp3, Caspase-1, and Gsdmd, in thyroid tissues. DAPI (blue) was used to counterstain nuclei. White arrowheads indicate positive cells for the respective proteins. (**D**–**F**) Quantitative analysis of the fluorescence intensity of Nlrp3, Caspase-1, and Gsdmd in thyroid tissues. Data are presented as mean ± SEM. All experiments were performed in triplicate. Statistical analysis was performed using one-way ANOVA followed by Tukey's post-hoc test. $^{**}P < 0.01$ (vs vehicle group), $^{\#\#}P < 0.01$ (vs 3 mg/kg CPF group), n = 6 per group.

Abbreviations: CPF, Chlorpyrifos; IF, Immunofluorescence; DAPI, 4′,6-diamidino-2-phenylindole; Nlrp3, NOD-like receptor protein 3; Gsdmd, Gasdermin D; SEM, Standard error of mean; ANOVA, Analysis of variance.

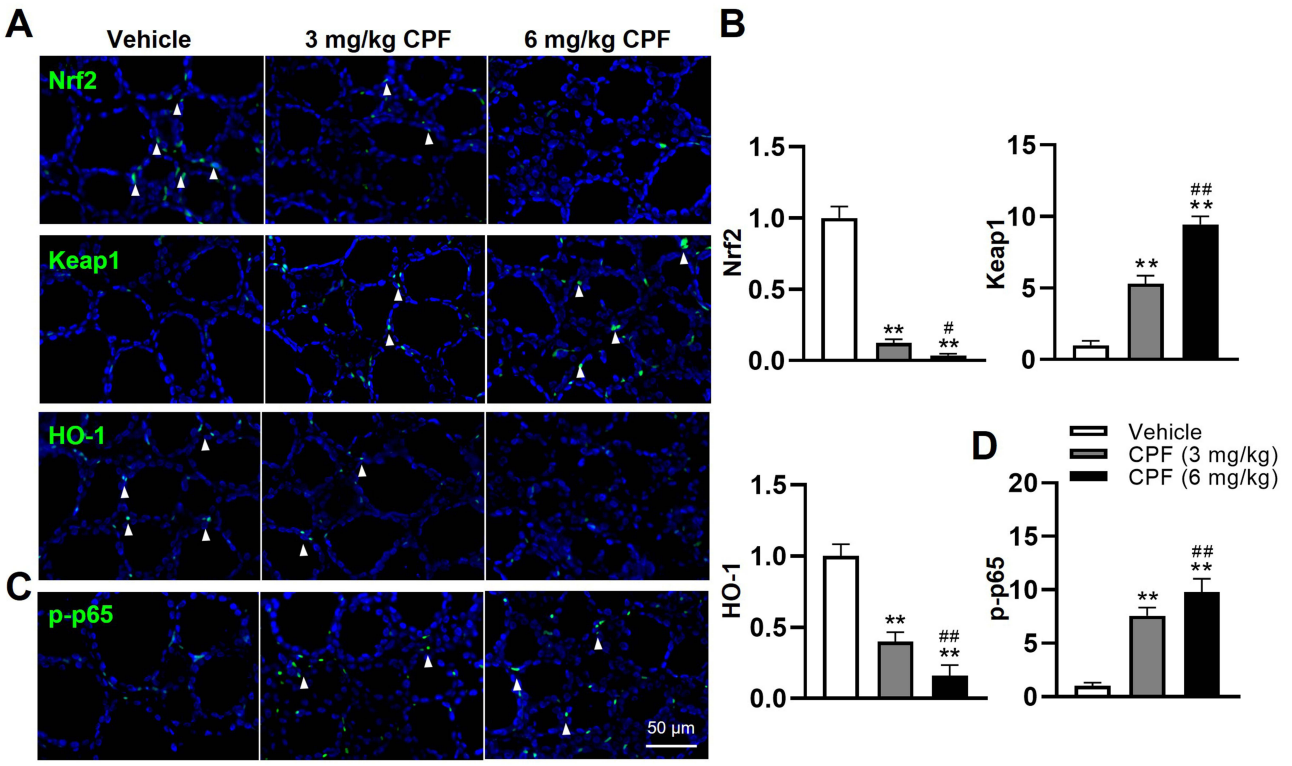

Figure 6 CPF exposure disrupts the Nrf2/Keap1 antioxidant pathway and activates NF-κB signaling in thyroid tissues. (**A** and **B**) Representative IF images (**A**) and quantitative analysis (**B**) of Nrf2, Keap1, and HO-1 expression in thyroid tissues. (**C** and **D**) Representative IF images (**C**) and quantitative analysis (**D**) of p-p65 expression in thyroid tissues. DAPI (blue) was used to counterstain nuclei. White arrowheads indicate positive cells for the respective proteins. Data are presented as mean ± SEM. All experiments were performed in triplicate. Statistical analysis was performed using one-way ANOVA followed by Tukey's post-hoc test. $^{**}P < 0.01$ (vs vehicle group), $^{\#}P < 0.05$, $^{\#\#}P < 0.01$ (vs 3 mg/kg CPF group), n = 6 per group.

Abbreviations: CPF, Chlorpyrifos; IF, Immunofluorescence; DAPI, 4′,6-diamidino-2-phenylindole; Nrf2, Nuclear factor erythroid 2-related factor 2; Keap1, Kelch-like ECH-associated protein 1; HO-1, Heme oxygenase-1; p-p65, phosphorylated p65; NF-κB, Nuclear factor kappa B; SEM, Standard error of mean; ANOVA, Analysis of variance.

https://doi.org/10.2147/JIR.S523861

Discussion

While the effects of CPF on thyroid hormones and structure have been previously documented,[18] the molecular mechanisms linking thyroid dysfunction to cellular pyroptosis remain poorly understood. In this study, we demonstrated that subchronic CPF exposure induced systemic toxicity in mice by reducing body weight and impairing serum overall antioxidant capacities, while causing significant damage to thyroid structure and endocrine function. Noteworthy, CPF exposure activated thyroid follicular cell pyroptosis by upregulating Nlrp3, Caspase-1, and Gsdmd proteins through the Nrf2/Keap1/NF-κB signaling axis in a dose-dependent manner (Figure 7). Our findings enhance our current understanding of CPF-induced thyrotoxicity, offering valuable insights into the detrimental consequences of long-term CPF exposure on thyroid homeostasis.

Toxicological studies have demonstrated that acute CPF administration at 10 mg/kg induces AChE inhibition and systemic toxicity, while lower doses (≤1 mg/kg) showed no significant clinical changes.[52] Moreover, subacute studies have further highlighted the dose-dependent effects of CPF exposure. For instance, Otênio et al (2022) reported that 10 mg/kg CPF administered orally to female Wistar rats for 5 days significantly damaged thyroid follicles with irregular contours and few or no colloids and led to a disorder of thyroid hormones.[18] Similarly, gestation CD-1 mice exposure to CPF at 3 and 6 mg/kg/day during gestational days 15–18, or postnatal exposure at 1 and 3 mg/kg/day during postnatal days 11–14, resulted in decreased T_4 levels and increased thyroid cell height in dams but significant reductions in follicular size, necrotic follicular cells, and lower serum T_4 levels in offspring, with male mice displaying greater susceptibility.[16] Besides, Chebab et al showed that continuous CPF exposure at 6.75 mg/kg for 30 days to sexually mature female Wistar rats significantly decreased serum T_3 and T_4 levels, along with significant body weight loss.[30] These findings indicate that CPF exerts cumulative and dose-dependent thyroid toxicity. Subsequently, research revealed that other soil contaminants such as microplastics and heavy metals can synergistically interact with CPF to amplify its toxicity.[53] Although environmental levels appear lower, the potential for bioaccumulation through multiple exposure routes justifies these doses as relevant for understanding both occupational exposure scenarios and chronic environmental accumulation, we herein selected two CPF doses (3 and 6 mg/kg) equivalent to 1/20 and 1/10 median lethal doses (LD_{50}) of mice,[45] as described in previous toxicological studies to elicit observable biological responses without severe systemic

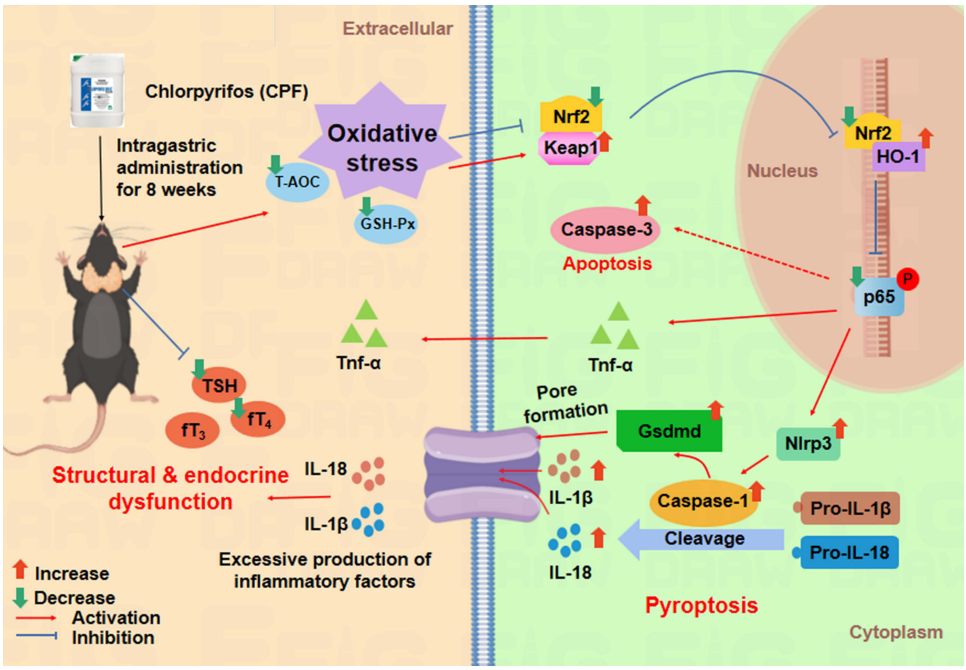

Figure 7 A schematic diagram illustrating how CPF exposure induces thyroid follicular cell pyroptosis and exacerbates thyrotoxicity by modulating the Nrf2/Keap1/NF-κB pathway.

Abbreviations: CPF, Chlorpyrifos; Nrf2, Nuclear factor erythroid 2-related factor 2; Keap1, Kelch-like ECH-associated protein 1; NF-κB, Nuclear factor kappa B.

toxicity.[16,43,44,46] Our findings further contribute to this body of knowledge by showing that sub-chronic CPF exposure disrupts thyroid structure and function in mice, emphasizing the toxic potential of CPF even at sub-lethal doses.

Previous studies have reported conflicting results regarding CPF's effects on thyroid hormone concentrations. For instance, a study using CD1 female mice (6 mg/kg CPF, 15–18 days) showed reduced serum T_4 levels,[16] while Otênio et al reported increased total T_3 levels in female Wistar rats treated with 0.01, 0.1, 1, or 10 mg/kg CPF for 5 days, but only treatment with 10 mg/kg CPF significantly increased fT_3 levels.[18] In our study, 8 weeks of CPF exposure to male mice revealed distinct patterns: significant reduction in fT_4 levels at 3 mg/kg and decreased TSH levels at 6 mg/kg, with no fT_3 changes, which may suggest that the toxicity of CPF could be realized by inducing hyperthyroidism and simultaneously impairment of negative feedback function of the hypothalamus and pituitary gland.[54] This contrasts with the transient increases in T_3 levels reported at higher CPF doses in previous studies, underscoring the complexity of CPF's dose-dependent effects on thyroid hormone regulation, suggesting that subchronic exposure, even at lower doses such as 3 mg/kg, can impair thyroid function and disrupt TSH feedback regulation. The observed discrepancies between studies highlight the need for standardized experimental designs, including consistent exposure regimens, animal models, and hormone measurement techniques, to resolve conflicting outcomes.

Our findings also highlight the role of pyroptosis, a form of programmed cell death mediated by the Nlrp3/Caspase-1 signaling pathway, in CPF-induced thyroid damage. Unlike apoptosis, which does not elicit an inflammatory response, pyroptosis is characterized by the release of pro-inflammatory cytokines such as IL-1β and IL-18.[55] We observed increased expression of pyroptosis-related key proteins (Nlrp3, Caspase-1, and Gsdmd) in thyroid tissues following CPF exposure, suggesting that CPF-induced thyrotoxicity is primarily driven by excessive inflammatory responses. Furthermore, proinflammatory factors like TNF- α and IL-1β, as the downstream of pyroptosis, may also contribute to apoptosis.[56] This dual pathway of cell death underscores the complexity of CPF-induced thyroid damage. These findings provide novel insights into the inflammatory mechanisms underlying CPF-induced thyrotoxicity and emphasize the need to consider both pyroptotic and apoptotic pathways when evaluating thyroid damage caused by environmental pollutants.

Oxidative stress plays a pivotal role in the pathogenesis of CPF-induced toxicity. Pyroptosis, a form of programmed cell death mediated by Nlrp3/Caspase-1 cascade, is closely associated with oxidative stress, with Nrf2/Keap1 pathway serving as a critical regulator of oxidative stress,[57] which can modulate Nlrp3-induced pyroptosis in acute lung injury,[58] porcine intestinal epithelial cells[59] and human bronchial epithelial cells.[60] Our latest findings also show that Nrf2-mediated thyroid follicular cell pyroptosis in cadmium-induced thyroid toxicity.[34] Aligning with these findings, our current results demonstrated for the first time that CPF induces thyroid pyroptosis through suppression of Nrf2/Keap1 antioxidative pathway and concurrent activation of NF-κB signaling. The downregulation of Nrf2 and its downstream effector HO-1, along with the upregulation of Keap1 and phosphorylated p65 (NF-κB), suggests that CPF disrupts the cellular antioxidative defense system, thereby promoting oxidative stress and inflammasome activation. This interplay between oxidative stress, Nrf2 suppression, and NF-κB activation creates a favorable environment for Nlrp3-mediated pyroptosis, exacerbating thyroid injury (Figure 7).

Despite the valuable insights gained from this study, several limitations should be acknowledged. First, thyroid hormones play a crucial role in promoting the growth and development of the organism. While our findings substantiated that CPF exposure could cause body weight loss and decreased fT_4 and TSH levels, fT_3 level remained unaffected. It remains unclear whether the observed body weight loss was primarily driven by CPF-induced decreases in thyroid hormones or by broader systemic toxicity caused by CPF exposure. Further studies are needed to clarify the specific contributions of thyroid dysfunction to CPF-induced weight loss. Second, we did not measure the CPF concentration in serum or thyroid tissue, which limits the better analysis of the cumulative burden of CPF in the body and its direct deposition in thyroid, precluding us from establishing a clearer relationship between CPF accumulation in thyroid tissue and the observed thyrotoxicity. Future studies employing tissue-specific CPF quantification would provide more direct evidence for CPF's localized effects on the thyroid. And considering the relatively small size of mice thyroid tissue, we may plan to adopt rats in subsequent experiments. Third, it remains unknown whether CPF exposure-induced body weight loss and thyrotoxicity are reversible following the cessation of exposure. While our study demonstrated CPF's effects on the Nrf2/Keap1/NF-κB pathway, we lack direct experimental evidence that pathway inhibition reduces pyroptosis. Future studies will employ pharmacological inhibitors (such as BAY 11–7082 for NF-κB or ML385 for

Nrf2) or gene knockout approaches to establish their causal role in CPF-induced thyroid toxicity. Additionally, investigating the recovery potential of thyroid function and systemic health after CPF withdrawal would be crucial to understanding the toxicity persistence. Future research will incorporate multiple time points post-withdrawal to evaluate tissue recovery and determine whether antioxidant or anti-inflammatory interventions could accelerate this process. Last, the exclusive use of male mice represents a limitation of our study. We selected male mice to minimize potential confounding effects from hormonal cycling, as the hypothalamic-pituitary-gonadal axis significantly influences thyroid function, particularly in females.[61,62] Previous studies suggest males may exhibit more susceptibility to CPF-induced neurotoxic effects, including cognitive deficits and behavioral changes, compared to females.[63,64] However, sex-specific differences in CPF-induced thyroid toxicity remain unexplored and warrant investigation. Future studies should include both sexes to comprehensively evaluate potential gender-dependent responses to CPF exposure and determine whether our findings are generalizable across the sexes. Consequently, our study focused exclusively on male mice. However, gender-specific effects of CPF exposure warrant further investigation, and future studies incorporating both sexes and various developmental stages will be crucial to elucidate gender-specific vulnerabilities and validate the broader applicability of our findings.

Conclusions

In summary, the present study highlights CPF's significant threat to thyroid structure and endocrine function, demonstrating its ability to induce thyroid pyroptosis via suppression of the Nrf2/Keap1 signaling pathway and activation of inflammatory responses. These findings deepen our understanding of CPF-induced thyroid toxicity and offer potential molecular targets for mitigating its harmful effects in clinical treatment. Moreover, they emphasize the need for stricter non-agricultural supervision of CPF usage and increased awareness of its risks among individuals in close contact with this pesticide.

Acknowledgments

This research was funded by Zhejiang Pharmaceutical Association Hospital Pharmacy Special Project (No. 2023ZYY11), the Joint Funds of the Zhejiang Provincial Natural Science Foundation of China under Grant No. BY24H290014, Traditional Chinese Medical Administration of Zhejiang Province (No. 2025ZL066), Zhejiang medical and health science and technology project (No. 2025KY098, 2024KY1216, and 2023KY235), Research Project of Zhejiang Chinese Medical University Scientific (No. 2023JKZKTS27 and 2023JKZKTS40), Research Project of Zhejiang Chinese Medical University Affiliated Hospital (No. 2023FSYYZY40, and 2023FSYYZZ02).

Disclosure

The authors report no conflicts of interest in this work.

References

1. Anwar S, Liaquat F, Khan QM, Khalid ZM, Iqbal S. Biodegradation of chlorpyrifos and its hydrolysis product 3,5,6-trichloro-2-pyridinol by bacillus pumilus strain C2A1. *J Hazard Mater*. 2009;168(1):400–405. doi:10.1016/j.jhazmat.2009.02.059
2. John EM, Shaike JM. Chlorpyrifos: pollution and remediation. *Environ Chem Lett*. 2015;13(3):269–291. doi:10.1007/s10311-015-0513-7
3. Huang X, Cui H, Duan W. Ecotoxicity of chlorpyrifos to aquatic organisms: a review. *Ecotoxicol Environ Saf*. 2020;200:110731. doi:10.1016/j.ecoenv.2020.110731
4. Arain M, Brohi M, Channa A, et al. Analysis of chlorpyrifos pesticide residues in surface water, ground water and vegetables through gas chromatography. *J Int Environ Appl Sci*. 2018;13:167.
5. Lockridge O, Verdier L, Schopfer LM. Half-life of chlorpyrifos oxon and other organophosphorus esters in aqueous solution. *Chem Biol Interact*. 2019;311:108788. doi:10.1016/j.cbi.2019.108788
6. Huang Y, Zhang W, Pang S, et al. Insights into the microbial degradation and catalytic mechanisms of chlorpyrifos. *Environ Res*. 2021;194:110660. doi:10.1016/j.envres.2020.110660
7. Bosu S, Rajamohan N, Al Salti S, Rajasimman M, Das P. Biodegradation of chlorpyrifos pollution from contaminated environment - a review on operating variables and mechanism. *Environ Res*. 2024;248:118212. doi:10.1016/j.envres.2024.118212
8. Amitai G, Moorad D, Adani R, Doctor BP. Inhibition of acetylcholinesterase and butyrylcholinesterase by chlorpyrifos-oxon. *Biochem Pharmacol*. 1998;56(3):293–299. doi:10.1016/s0006-2952(98)00035-5
9. Eaton DL, Daroff RB, Autrup H, et al. Review of the toxicology of chlorpyrifos with an emphasis on human exposure and neurodevelopment. *Crit Rev Toxicol*. 2008;38(2):1–125. doi:10.1080/10408440802272158

10. Gallegos CE, Bartos M, Gumilar F, Minetti A, Baier CJ. Behavioral and neurochemical impairments after intranasal administration of chlorpyrifos formulation in mice. *Pestic Biochem Physiol*. 2023;189:105315. doi:10.1016/j.pestbp.2022.105315
11. Rodriguez PM, Vera B, Burgos C, et al. Expression of carboxylesterase and paraoxonase in the placenta and their association with chlorpyrifos exposure during pregnancy. *Ecotoxicol Environ Saf*. 2025;298:118285. doi:10.1016/j.ecoenv.2025.118285
12. Ramos Nieto MR, Lasagna M, Cao G, et al. Chronic exposure to low concentrations of chlorpyrifos affects normal cyclicity and histology of the uterus in female rats. *Food and Chemical Toxicology*. 2021;156:112515. doi:10.1016/j.fct.2021.112515
13. Umosen AJ, Ambali SF, Ayo JO, Mohammed B, Uchendu C. Alleviating effects of melatonin on oxidative changes in the testes and pituitary glands evoked by subacute chlorpyrifos administration in Wistar rats. *Asian Pac J Trop Biomed*. 2012;2(8):645–650. doi:10.1016/S2221-1691(12)60113-0
14. Tanvir EM, Afroz R, Chowdhury M, et al. A model of chlorpyrifos distribution and its biochemical effects on the liver and kidneys of rats. *Hum Exp Toxicol*. 2016;35(9):991–1004. doi:10.1177/0960327115614384
15. Brandt C, Burnett DC, Arcinas L, Palace V, Gary Anderson W. Effects of chlorpyrifos on in vitro sex steroid production and thyroid follicular development in adult and larval lake sturgeon, Acipenser fulvescens. *Chemosphere*. 2015;132:179–187. doi:10.1016/j.chemosphere.2015.03.031
16. De Angelis S, Tassinari R, Maranghi F, et al. Developmental Exposure to Chlorpyrifos Induces Alterations in Thyroid and Thyroid Hormone Levels Without Other Toxicity Signs in Cd1 Mice. *Toxicological Sciences*. 2009;108(2):311–319. doi:10.1093/toxsci/kfp017
17. ResearchGate. (PDF) The propolis effect on chlorpyrifos induced thyroid toxicity in male albino rats. 2024. Available from: https://www.researchgate.net/publication/318678368_The_Propolis_Effect_on_Chlorpyrifos_Induced_Thyroid_Toxicity_in_Male_Albino_Rats. Accessed 19, February, 2025.
18. Otênio JK, Souza KD, Alberton O, et al. Thyroid-disrupting effects of chlorpyrifos in female Wistar rats. *Drug Chem Toxicol*. 2022;45(1):387–392. doi:10.1080/01480545.2019.1701487
19. Mansukhani M, Roy P, Ganguli N, Majumdar SS, Sharma SS. Organophosphate pesticide chlorpyrifos and its metabolite 3,5,6-trichloropyridinol downregulate the expression of genes essential for spermatogenesis in caprine testes. *Pestic Biochem Physiol*. 2024;204:106065. doi:10.1016/j.pestbp.2024.106065
20. Ventura C, Zappia CD, Lasagna M, et al. Effects of the pesticide chlorpyrifos on breast cancer disease. Implication of epigenetic mechanisms. *J Steroid Biochem Mol Biol*. 2019;186:96–104. doi:10.1016/j.jsbmb.2018.09.021
21. Guo J, Zhang J, Wu C, et al. Associations of prenatal and childhood chlorpyrifos exposure with neurodevelopment of 3-year-old children. *Environ Pollut*. 2019;251:538–546. doi:10.1016/j.envpol.2019.05.040
22. Zheng R, Romero-Del Rey R, Ruiz-Moreno F, et al. Depressive symptoms and suicide attempts among farmers exposed to pesticides. *Environ Toxicol Pharmacol*. 2024;108:104461. doi:10.1016/j.etap.2024.104461
23. Bryliński Ł, Kostelecka K, Woliński F, et al. Effects of trace elements on endocrine function and pathogenesis of thyroid diseases-a literature review. *Nutrients*. 2025;17(3):398. doi:10.3390/nu17030398
24. Hoermann R, Midgley JEM, Larisch R, Dietrich JW. Recent advances in thyroid hormone regulation: toward a new paradigm for optimal diagnosis and treatment. *Front Endocrinol*. 2017;8:364. doi:10.3389/fendo.2017.00364
25. Najjar F, Milbauer L, Wei CW, Lerdall T, Wei LN. Modelling Functional Thyroid Follicular Structures Using P19 Embryonal Carcinoma Cells. *Cells*. 2024;13(22):1844. doi:10.3390/cells13221844
26. Barr DB, Allen R, Olsson AO, et al. Concentrations of selective metabolites of organophosphorus pesticides in the United States population. *Environ Res*. 2005;99(3):314–326. doi:10.1016/j.envres.2005.03.012
27. Liem JF, Subekti I, Mansyur M, et al. The determinants of thyroid function among vegetable farmers with primary exposure to chlorpyrifos: a cross-sectional study in central java, Indonesia. *Heliyon*. 2023;9(6):e16435. doi:10.1016/j.heliyon.2023.e16435
28. Kongtip P, Nankongnab N, Pundee R, et al. Acute changes in thyroid hormone levels among Thai pesticide sprayers. *Toxics*. 2021;9(1):16. doi:10.3390/toxics9010016
29. Akande MG, Shittu M, Uchendu C, Yaqub LS. Taurine ameliorated thyroid function in rats co-administered with chlorpyrifos and lead. *Vet Res Commun*. 2016;40(3–4):123–129. doi:10.1007/s11259-016-9662-9
30. Chebab S, Mekircha F, Leghouchi E. Potential protective effect of Pistacia lentiscus oil against chlorpyrifos-induced hormonal changes and oxidative damage in ovaries and thyroid of female rats. *Biomed Pharmacother*. 2017;96:1310–1316. doi:10.1016/j.biopha.2017.11.081
31. Peluso T, Nittoli V, Reale C, et al. Chronic exposure to chlorpyrifos damages thyroid activity and imbalances hepatic thyroid hormones signaling and glucose metabolism: dependency of T3-FOXO1 axis by hyperglycemia. *Int J Mol Sci*. 2023;24(11):9582. doi:10.3390/ijms24119582
32. Spirhanzlova P, Couderq S, Le Mével S, et al. Short- and long-term effects of chlorpyrifos on thyroid hormone axis and brain development in xenopus laevis. *Neuroendocrinology*. 2023;113(12):1298–1311. doi:10.1159/000525719
33. Qiao K, Hu T, Jiang Y, et al. Crosstalk of cholinergic pathway on thyroid disrupting effects of the insecticide chlorpyrifos in zebrafish (danio rerio). *Sci Total Environ*. 2021;757:143769. doi:10.1016/j.scitotenv.2020.143769
34. Chen Y, Zhou C, Bian Y, et al. Cadmium exposure promotes thyroid pyroptosis and endocrine dysfunction by inhibiting Nrf2/Keap1 signaling. *Ecotoxicol Environ Saf*. 2023;249:114376. doi:10.1016/j.ecoenv.2022.114376
35. Zhao X, Luo H, Yao S, et al. Atrazine exposure promotes cardiomyocyte pyroptosis to exacerbate cardiotoxicity by activating NF-κB pathway. *Sci Total Environ*. 2024;915:170028. doi:10.1016/j.scitotenv.2024.170028
36. Ge Y, Chen Y, Guo C, et al. Pyroptosis and intervertebral disc degeneration: mechanistic insights and therapeutic implications. *J Inflammation Res*. 2022;15:5857–5871. doi:10.2147/JIR.S382069
37. Liu J, Mao C, Dong L, et al. Excessive iodine promotes pyroptosis of thyroid follicular epithelial cells in hashimoto's thyroiditis through the ROS-NF-κB-NLRP3 pathway. *Front Endocrinol*. 2019;10:778. doi:10.3389/fendo.2019.00778
38. Jang Y, Lee AY, Jeong SH, et al. Chlorpyrifos induces NLRP3 inflammasome and pyroptosis/apoptosis via mitochondrial oxidative stress in human keratinocyte HaCaT cells. *Toxicology*. 2015;338:37–46. doi:10.1016/j.tox.2015.09.006
39. Miao Z, Miao Z, Teng X, Xu S. Chlorpyrifos triggers epithelioma papulosum cyprini cell pyroptosis via miR-124-3p/CAPN1 axis. *J Hazard Mater*. 2022;424(Pt A):127318. doi:10.1016/j.jhazmat.2021.127318
40. Fu F, Luo H, Du Y, et al. AR/PCC herb pair inhibits osteoblast pyroptosis to alleviate diabetes-related osteoporosis by activating Nrf2/Keap1 pathway. *J Cell Mol Med*. 2023;27(22):3601–3613. doi:10.1111/jcmm.17928
41. Zhao MW, Yang P, Zhao LL. Chlorpyrifos activates cell pyroptosis and increases susceptibility on oxidative stress-induced toxicity by miR-181/SIRT1/PGC-1α/Nrf2 signaling pathway in human neuroblastoma SH-SY5Y cells: implication for association between chlorpyrifos and Parkinson's disease. *Environ Toxicol: Int J*. 2019;34(6):699–707. doi:10.1002/tox.22736

42. Abduh MS, Alruhaimi RS, Alqhtani HA, et al. Rosmarinic acid mitigates chlorpyrifos-induced oxidative stress, inflammation, and kidney injury in rats by modulating SIRT1 and Nrf2/HO-1 signaling. *Life Sci*. 2023;313:121281. doi:10.1016/j.lfs.2022.121281
43. Zhu R, Tong X, Du Y, et al. Improvement of chlorpyrifos-induced cognitive impairment by mountain grape anthocyanins based on PI3K/akt signaling pathway. *Pestic Biochem Physiol*. 2024;205:106172. doi:10.1016/j.pestbp.2024.106172
44. Sharifnia M, Eftekhari Z, Mortazavi P. Niosomal hesperidin attenuates the M1/M2-macrophage polarization-based hepatotoxicity followed chlorpyrifos -induced toxicities in mice. *Pestic Biochem Physiol*. 2024;198:105724. doi:10.1016/j.pestbp.2023.105724
45. El-Sebae AH, Ahmed NS, Soliman SA. Effect of pre-exposure on acute toxicity of organophosphorus insecticides to white mice. *J Environ Sci Health, B Pestic Food Contam Agric Wastes*. 1978;13(1):11–24. doi:10.1080/03601237809372074
46. Ma P, Wu Y, Zeng Q, et al. Oxidative damage induced by chlorpyrifos in the hepatic and renal tissue of Kunming mice and the antioxidant role of vitamin E. *Food Chem Toxicol Int J Publ Br Ind Biol Res Assoc*. 2013;58:177–183. doi:10.1016/j.fct.2013.04.032
47. Ellison CA, Smith JN, Lein PJ, Olson JR. Pharmacokinetics and pharmacodynamics of chlorpyrifos in adult male long-Evans rats following repeated subcutaneous exposure to chlorpyrifos. *Toxicology*. 2011;287(1–3):137–144. doi:10.1016/j.tox.2011.06.010
48. Farahat FM, Ellison CA, Bonner MR, et al. Biomarkers of chlorpyrifos exposure and effect in Egyptian cotton field workers. *Environ Health Perspect*. 2011;119(6):801–806. doi:10.1289/ehp.1002873
49. Lee YS, Lewis JA, Ippolito DL, et al. Repeated exposure to neurotoxic levels of chlorpyrifos alters hippocampal expression of neurotrophins and neuropeptides. *Toxicology*. 2016;340:53–62. doi:10.1016/j.tox.2016.01.001
50. Rohlman DS, Anger WK, Lein PJ. Correlating neurobehavioral performance with biomarkers of organophosphorous pesticide exposure. *Neurotoxicology*. 2011;32(2):268–276. doi:10.1016/j.neuro.2010.12.008
51. Santos BR, Cordeiro JMDA, Santos LC, da Santana LS, de Nascimento AEJ, Silva JF. Kisspeptin suppresses inflammasome-NLRP3 activation and pyroptosis caused by hypothyroidism at the maternal-fetal interface of rats. *Int J Mol Sci*. 2023;24(7):6820. doi:10.3390/ijms24076820
52. European FSA (EFSA). Conclusion on the peer review of the pesticide risk assessment of the active substance glyphosate. *EFSA J*. 2015;13 (11):4302. doi:10.2903/j.efsa.2015.4302.
53. Fu J, Chen X, Li J, Peng L. Thyroid hormones and prognosis in adults with status epilepticus: a retrospective study. *Front Endocrinol*. 2024;15:1452299. doi:10.3389/fendo.2024.1452299
54. Surks MI, Ortiz E, Daniels GH, et al. Subclinical thyroid disease: scientific review and guidelines for diagnosis and management. *JAMA*. 2004;291 (2):228–238. doi:10.1001/jama.291.2.228
55. Bertheloot D, Latz E, Franklin BS. Necroptosis, pyroptosis and apoptosis: an intricate game of cell death. *Cell Mol Immunol*. 2021;18 (5):1106–1121. doi:10.1038/s41423-020-00630-3
56. Yin L, Dai Q, Jiang P, et al. Manganese exposure facilitates microglial JAK2-STAT3 signaling and consequent secretion of TNF-a and IL-1β to promote neuronal death. *Neurotoxicology*. 2018;64:195–203. doi:10.1016/j.neuro.2017.04.001
57. Li C, Cheng L, Wu H, et al. Activation of the KEAP1-NRF2-ARE signaling pathway reduces oxidative stress in Hep2 cells. *Mol Med Rep*. 2018;18 (3):2541–2550. doi:10.3892/mmr.2018.9288
58. Zhang Q, Zeng M, Zhang B, et al. Salvianolactone acid a isolated from salvia miltiorrhiza ameliorates lipopolysaccharide-induced acute lung injury in mice by regulating PPAR-γ. *Phytomed*. 2022;105:154386. doi:10.1016/j.phymed.2022.154386
59. Qiu M, Hao Z, Liu Y, et al. ROS acted as an initial role in selenium nanoparticles alleviating insecticide chlorpyrifos-induced oxidative stress, pyroptosis, and intestinal barrier dysfunction in porcine intestinal epithelial cells. *Pestic Biochem Physiol*. 2025;211:106418. doi:10.1016/j.pestbp.2025.106418
60. J B, G S, Y X, et al. The role of HMGB1 on TDI-induced NLPR3 inflammasome activation via ROS/NF-κB pathway in HBE cells. *Int Immunopharmacol*. 2021:98. doi:10.1016/j.intimp.2021.107859.
61. Brown EDL, Obeng-Gyasi B, Hall JE, Shekhar S. The thyroid hormone axis and female reproduction. *Int J Mol Sci*. 2023;24(12):9815. doi:10.3390/ijms24129815
62. Tammaro A, Lori G, Martinelli A, Cancemi L, Tassinari R, Maranghi F. Risk assessment of transgender people: implementation of a demasculinizing-feminizing rodent model including the evaluation of thyroid homeostasis. *Biol Direct*. 2024;19(1):5. doi:10.1186/s13062-023-00450-1
63. Venerosi A, Tait S, Stecca L, et al. Effects of maternal chlorpyrifos diet on social investigation and brain neuroendocrine markers in the offspring - a mouse study. *Environ Health Glob Access Sci Source*. 2015;14:32. doi:10.1186/s12940-015-0019-6
64. Silva MH. Effects of low-dose chlorpyrifos on neurobehavior and potential mechanisms: a review of studies in rodents, zebrafish, and Caenorhabditis elegans. *Birth Defects Res*. 2020;112(6):445–479. doi:10.1002/bdr2.1661